Colloid Polym Sci 274:826–835 (1996)


ORIGINAL CONTRIBUTION

F. Stieber
H.-F. Eicke

# Solution of telechelic ionomers in water/AOT/oil (w/o) microemulsions: a static and dynamic light scattering study

Received: 15 December 1995
Accepted: 1 March 1996

F. Stieber · Prof. Dr. H.-F. Eicke (✉)
Institut für Physikalische Chemie
Department Chemie
Universität Basel
Klingelbergstraße 80
4056 Basel, Switzerland

**Abstract** Static and quasielastic light-scattering measurements of end-sulfonated polyisoprene in a water in oil (w/o) microemulsions were used to characterize the structure and diffusion properties of this complex system. The hydrophilic end groups of the polymer stick to the surfactant covered oil/water interface, thus bridging the water droplets. This structure formation decreases the mobility of the aqueous nanodroplets and polymer molecules. At inter-droplet distances larger than the end-to-end distance of the ionomer chain a decrease of the osmotic modulus is observed. It can be explained by a depletion force of free ionomer chains acting on the nano-droplets. With increasing polymer concentration structure formation of the microemulsion is observed at nanodroplet concentrations where the ionomer chains just fit the average separation of two nanodroplets.

**Key words** Telechelic ionomers – light scattering – transient network – w/o microemulsions

## Introduction

Interactions between polymers and organized surfactant systems are of considerable interest from a scientific and industrial point of view. Aqueous solutions of such systems are studied in great detail which is reviewed in [1]. Polymer–surfactant complexes formed in apolar solvents are hardly studied [2]. Microemulsions might well be considered as a particular class of solvents having a compartmentalized structure of hydrophilic and hydrophobic domains on a nanometer scale separated by a surfactant monolayer. Functionalized polymers consisting of hydrophilic and hydrophobic blocks show structure formation in such "complex" solvents by trying to accommodate these blocks in the apolar and polar domain. In a series of papers, we reported on structural and dynamic properties of ABA triblock-copolymers in AOT/water/isooctane w/o microemulsions [3–5]. The observed "core-shell" structure and dimerization of microemulsion droplets at small polymer concentrations (approximately one polymer per nanodroplet) [3], the large viscosity enhancement and viscoelastic behavior at higher polymer concentration [4] and the slow diffusion process measured by quasielastic light scattering (QELS) [5] result from the particular chemical structure of the copolymer and microemulsion, respectively. Reversible bridging of colloidal particles by blockcopolymers or telechelic ionomers gives rise to transient networks with interesting dynamic and rheologic properties [6]. These properties depend on the thermodynamics of the polymer chain and on the chain dynamics in the vicinity of the interface. Recent theoretical work focused on the nature of transient networks formed by polymers with sticky end groups or blocks [7–9].

In this paper, we report on static and dynamic light scattering measurements of telechelic ionomers in w/o microemulsions. In contrast to blockcopolymers the interactions of the ionomer chain with the hydrophilic nanodroplets is much weaker, i.e., the strength of the transient

networks is diminished. This is a consequence of the hydrophilic end groups being localized in the surfactant layer. Upon addition of ionomers, hence, the droplet properties, i.e., size and refractive index, are not changed and the exchange of polymers between different droplets does not disturb the surfactant layer. This facilitates the analysis of the light scattering measurements since the scattered light stems almost exclusively from the nanodroplet whose molecular weight exceeds by far that of the ionomer. Additionally, it is possible to change the refractive index of the oil phase to match the ionomer chain which yields information on the nature of the observed diffusive processes.

## Experimental

### Materials

Water in oil microemulsions were prepared from AOT, (sodium bis (2-ethylhexyl) sulfosuccinate), obtained commercially in microselect quality from Fluka, *n*-octane (Fluka) or dipentene (Fluka) and water, deionized with the Alpha-Q-Reagent Grade system (Millipore). The composition of the microemulsion corresponds to the optically transparent and low viscous mono-phasic region within the ternary phase diagram and is characterized by a molar ratio of water to AOT, i.e., here $w_0 = 62$ corresponding to the mass ratio of water to AOT $r_w = 2.5$. Assuming a mean polar head group area in the water/oil interface of $5.8\ 10^{-19}\ m^2$ [10] a droplet radius $r_{nd} = 9.6$ nm and a molecular mass $M_{nd} = 3.2\ 10^6$ g/mol are calculated.

The ionomer used consists of a polyisoprene chain with sodium sulfonate end groups. The synthesis is described elsewhere [11]. The molecular weight $M_w$ of the polyisoprene chain is 50 000 g/mol and the polydispersity $M_w/M_n = 1.08$.

We use a complex solvent, i.e., a three-component microemulsion characterized by the size ($r_{nd}$) and the concentration of nanodroplets ($c_{nd}$) . The droplet size is kept constant. Another important parameter is the polymer concentration ($c_p$) expressed by the mass of polymer per volume of oil. It adjusts the chain segment density independent of the nanodroplet concentration, since the polymer chains are oil compatible. A third parameter is the number of polymer molecules per nanodroplet, $R$. It determines the functionality of the nanodroplets and is relevant for network formation. $R$ is related to $c_p$ and $c_{nd}$ and cannot be chosen independently of these concentrations. We have changed, therefore, first the polymer concentration at constant $c_{nd}$ (series A and B), i.e., the number of polymer molecules per nanodroplet $R$ increases with increasing $c_p$. Secondly, three series were prepared by dilution at constant $c_p$ (series C, D, E), i.e., $R$ increases with decreasing $c_{nd}$. For a particular concentration dipentene, which is also a good solvent for polyisoprene, instead of *n*-octane was used as the oil phase. The refractive index of dipentene is $n = 1.47$, this is close to that of PI ($n = 1.51$) in contrast to $n = 1.39$ of *n*-octane.

The sample characteristics are listed in Table 1.

The overlap concentration $c^*$ of a polymer chain in solution can be estimated from $c^* = M/(N_A r_g^3)$ . $N_A$ being Avogadro's constant and $r_g$ the radius of gyration [12]. From the radius of gyration, we find $c^* = 0.041$ g/cm$^3$ in a good solvent. Our experimental $c_p$ values are smaller than 0.026 g/cm$^3$, hence, the solution of the PI chains in the oil phase is dilute. The end-to-end distance of the PI chain in a good solvent is approximately 32 nm [13].

### Light scattering

The static and dynamic light scattering experiments were performed using a commercial goniometer (ALV-Langen)

**Table 1**

| series | |
|---|---|
| A<br>$c_{nd} = 0.157$ g/cm$^{-3}$ | $c_p = \{0.056, 0.033, 0.021, 0.011, 0.005\}$ g/cm$^{-3}$<br>$R = \{10, 5.7, 3.7, 1.9, 0.8\}$ |
| B<br>$c_{nd} = 0.15$ g/cm$^{-3}$ | $c_p = \{0.026, 0.016, 0.011, 0.0055\}$ g/cm$^{-3}$<br>$R = \{9.6, 6.0, 4.0, 2.0\}$ |
| C<br>$c_p = 0.003$ g/cm$^{-3}$ | $c_{nd} = \{0.158, 0.153, 0.19, 0.15, 0.11, 0.072, 0.037, 0.018\}$ g/cm$^{-3}$<br>$R = \{0.5, 0.63, 0.8, 1.1, 1.5, 2.4, 4.9, 10.5\}$ |
| D<br>$c_p = 0.007$ g/cm$^{-3}$ | $c_{nd} = \{0.158, 0.153, 0.19, 0.15, 0.11, 0.072, 0.054, 0.045\}$ g/cm$^{-3}$<br>$R = \{1.2, 1.5, 1.9, 2.5, 3.6, 5.7, 7.8, 9.5\}$<br>$c_{nd} = \{0.039, 0.038, 0.037, 0.028, 0.018\}$ g/cm$^{-3}$<br>$R = \{10.9, 11.3, 11.7, 15.1, 24.4\}$ |
| E<br>$c_p = 0.021$ g/cm$^{-3}$ | $c_{nd} = \{0.157, 0.153, 0.19, 0.15, 0.11, 0.071, 0.036\}$ g/cm$^{-3}$<br>$R = \{3.6, 4.6, 5.8, 7.8, 11.1, 17.5, 35.8\}$ |

Colloid & Polymer Science, Vol. 274, No. 9 (1996)


equipped with a frequency doubled NdYAg-laser (ADLAS, wavelength $\lambda = 532$ nm) at scattering angles $\theta$ between 20° and 150°. Thus, the scattering vector $q = 2\pi n/\lambda \sin(\theta/2)$ varies between 5.7 $10^6$ and 3.2 $10^7$ $m^{-1}$. An ALV-5000/E correlator was at our disposal to calculate the photon intensity autocorrelation function $g^2(t)$. The samples were prepared by filtering them through a Millipore filter (FGS, 0.2 $\mu$m) into 10 mm o.d. quartz cells. They were plugged up by a long Teflon stopper which reduces the gas volume above the sample to minimize evaporation of the oil. Prior to the measurements the cells were homogenized by rolling them for a few hours on a rock'n roller table at the measuring temperature. The sample cell housing mounted in an optical matching vat is temperature controlled to $T \pm 0.02$ K. Data analysis was performed on the normalized intensity autocorrelation function $g^2(t)$ using a non-linear regularization method performed by the ALV-800 transputer. Selected data series were fitted to a double stretched exponential function using a nonlinear least square fitting routine.

The time averaged scattered light intensity is expressed by $Kc/R_\theta$, with an optical contrast factor $K = 4\pi^2 n_0^2/\lambda^4 \, (dn/dc)^2$, $n_0$ being the refractive index of the solution, $c$ the concentration of nanodroplets in g/cm$^3$ and $R_\theta$ the Rayleigh ratio of the solution corrected for the scattering contribution of the pure solvent. The refractive index increment $dn/dc$ was measured at 20 °C using a Brice Phoenix differential refractometer.

### Conductivity

The conductivity was determined using an autobalanced conductivity bridge CDM-83, operating for optimum sensitivity between 70 Hz and 50 kHz depending on the conductivity range. The sample cell containing the platinum electrodes was thermostated to $T \pm 0.02$ K.

### Viscosity

The viscosity was measured using a thermostated Ubbelohde capillary viscosimeter.

## Results

### Constant interdroplet distance

The effect of the ionomer on the phase diagram is hardly observable in the concentration range investigated. This is in contrast to our w/o-microemulsions with triblock-copolymer where the mono-phasic region of the polymer-microemulsion systems is broadened [4], apparently due to the interaction of the POE chains with the nanodroplets [14]. Still the ionic end groups must be essential for the thermodynamic stability of the system: the PI blocks of the same molecular weight as the ionomer, however, with hydrophobic end groups cannot be dissolved even at concentrations lower than $10^{-3}$ g/cm$^3$ in the microemulsion without phase separation. This is explained by the action of a depletion force between the nanodroplets caused by an osmotic pressure difference of the polymer chains in the gap between neighboring droplets and outside this gap [15].

Typical angular dependent intensity correlation functions at $c_{nd} = 0.15$ and 0.27 and $R = 4$ are shown in Fig. 1. Two correlation processes can be distinguished. The amplitude of the slow decay decreases with increasing scattering vector. Both, the nonlinear regularization analysis and the nonlinear least square fit of two stretched exponential functions yield a $q^2$-dependence of the correlation rate for the fast and slow process, indicating the diffusive character

**Fig. 1** Auto correlation function obtained from QELS at different scattering angles for $R = 4$ and $c_{nd} = 0.15$ g/cm$^3$ (upper curves) and $c_{nd} = 0.27$ g/cm$^3$ (lower curves) at $T = 15$ °C

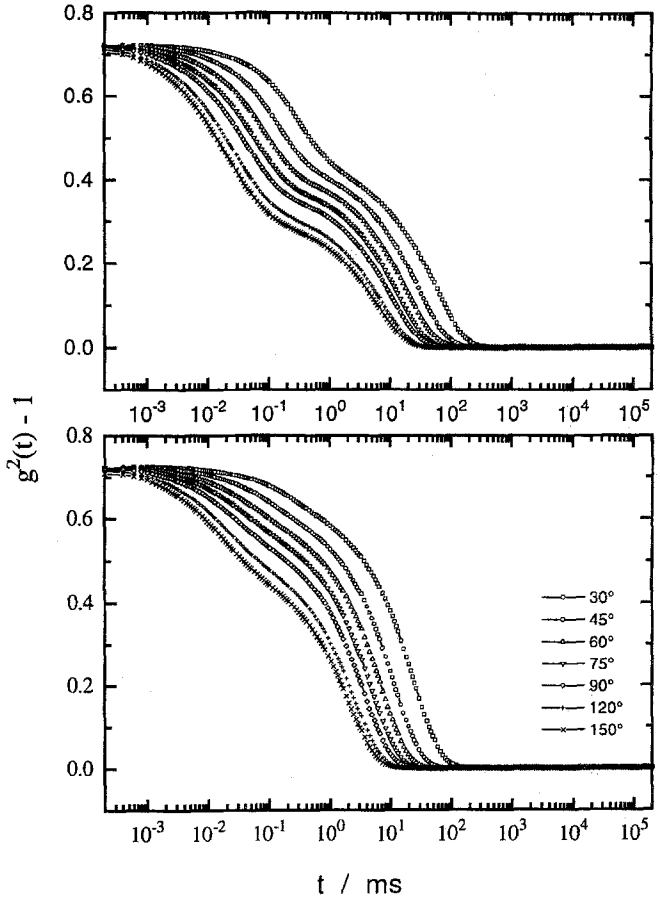

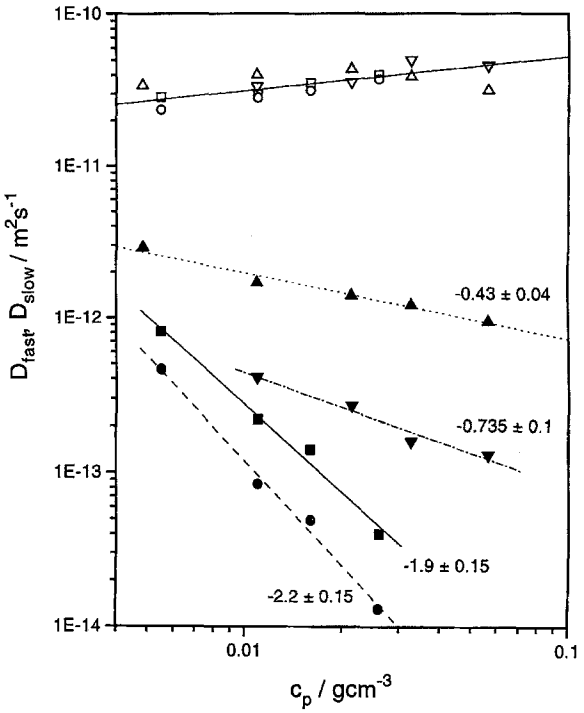


**Fig. 2** Diffusion coefficients (obtained from the fit of two stretched exponential functions to the autocorrelation function) against the polymer concentration. Open symbols correspond to the fast diffusion process, closed symbols to the slow process. ($c_{nd} = 0.15$ g/cm$^3$: ■ □ $T = 20$ °C, ● ○$T = 15$ °C; $c_{nd} = 0.27$ g/cm$^3$; ▲ △ $T = 20$ °C, ▼ ▽ $T = 15$ °C). The numbers indicate the power law exponents

of these processes. The dependence of the diffusion constants on the polymer concentration is shown in Fig. 2 for series A and B. The fast diffusion is only weakly concentration dependent, however, becomes faster with increasing $c_p$. The slow process behaves quite differently regarding the two droplet concentrations: for $c_{nd} = 0.15$ g/cm$^3$ the slope in a log-log plot is about $-2$ and almost temperature independent. For $c_{nd} = 0.27$ g/cm$^3$ the slope becomes smaller and strongly temperature dependent. This temperature behaviour is replotted in detail at constant $R$ in Fig. 3. To elucidate this temperature effect we show the temperature-dependent conductivity for both nanodroplet concentrations (see inset). At $c_{nd} = 0.27$ g/cm$^3$ the onset of a system spanning nanodroplet cluster occurs revealed by an increase of the conductivity over several orders of magnitude. For $c_{nd} = 0.15$ g/cm$^3$ only a very weak temperature dependence is observed. This transition at the higher concentration is characterized by a dynamic clustering of droplets which is a well known property of microemulsions [16]. At our particular droplet size and concentration this dynamic droplet cluster consists of individual droplets which are temporarily in contact with each other by the aliphatic AOT tails. This contact increases drastically the electrical conductivity via an improved sodium and surfactant ion exchange between the nanodroplets. The dynamical droplet clustering markedly increases the slow diffusion coefficient (by a factor of about 5). Please note that the collective diffusion coefficient in the pure microemulsion and the fast diffusion process in the polymer containing samples are almost not affected by the system spanning droplet cluster. This is a consequence of its dynamic character.

Figure 4 shows the angular dependent correlation functions for $c_{nd} = 0.072$ g/cm$^3$ and $R = 5.7$ using dipentene and *n*-octane. In contrast to *n*-octane matching of the polymer in dipentene leads to a suppression of the slow diffusion process.

## Constant polymer concentration

In order to calculate $Kc/R_\theta$, one has to calculate the optical contrast factor $K$ and, therefore, one has to know the refractive index increment for the scattering system. In our case the scattering systems consist of droplets which can be treated as hard sphere scatterers and polymer chains added to the solution of these spheres without interpenetrating the spheres. Due to the low molecular weight of the polymer chains compared to the nanodroplets, their dynamics is much faster. Thus, one can treat the spheres as scatterers in a background medium of oil and polymer chains. In other words the optical contrast factor is determined by the refractive index increment of the nanodroplets with respect to the polymer solution rather than the pure oil. Furthermore, the scattered light intensity of the nanodroplets is by a factor of 1000 larger than the scattered light intensity of the polymer chains at the lowest droplet concentration and largest polymer concentration, which is caused by their large difference in molecular weight inspite of the larger refractive index increment of the polymer solution. We have measured the refractive index difference between the series with constant polymer concentration and the pure polymer solution and obtained $dn/dc = -0.0277$ ml/g $- 0.1$ ml$^2$/g$^2$ $c_p$. It is obvious that adding the polymer to the oil increases the difference of the refractive indices of the nanodroplets and the polymer solution, therefore slightly increasing the absolute value of the refractive index increment. The above arguments holds only if there occurs no clustering of droplets and polymer chains. This case will be discussed below. In the case of the lowest $c_p$ the influence of the polymer on the value of $dn/dc$ is completely negligible.

We now present light scattering data of the series C, D, E where $c_{nd}$ was changed at constant $c_p$. For comparison the proper microemulsions without polymer were studied at different droplet concentrations. Series D displayed

Colloid & Polymer Science, Vol. 274, No. 9 (1996)


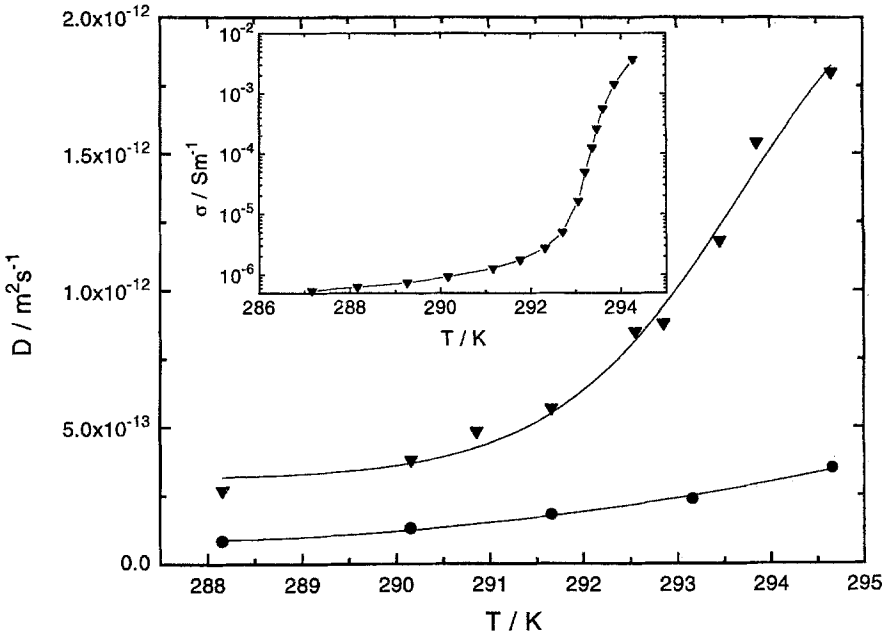


**Fig. 3** Slow diffusion coefficient against temperature for $c_{nd}$ = 0.15 g/cm$^3$ (●) and $c_{nd}$ = 0.27 g/cm$^3$ (▼) at $R = 4$. The inset shows the temperature dependent conductivity for $c_{nd}$ = 0.27 g/cm$^3$

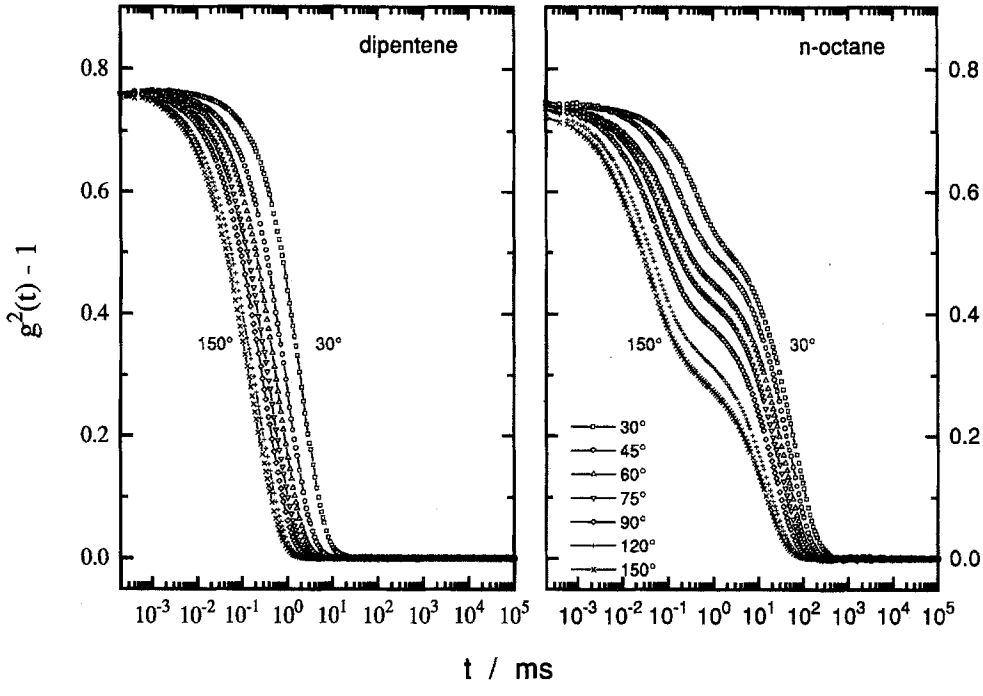


**Fig. 4** Auto correlation function obtained from QELS at different scattering angles for $R = 5.7$ using dipentene (left curves) and *n*-octane (right curves) as continuous oil phases

a strange scattering behavior as shown in Fig. 5. For $c_{nd} > 0.1$ g/cm$^3$ a monotonically decreasing value of $Kc/R_\theta$ was found almost independent of $q^2$. At still lower concentrations an increasing angular dependence of the scattered light is observed and within a narrow concentration range of 0.025 to 0.04 g/cm$^3$ a strong increase of $Kc/R_\theta$ occurred. Extrapolation of $Kc/R_\theta$ to $q = 0$ yields the osmotic modulus $(RT)^{-1}\delta\pi/\delta c$, a thermodynamic quantity which is plotted against the nanodroplet concentrations for the C, D and E series and the pure microemulsion. At high droplet concentrations a monotonic increase of the osmotic modulus with increasing polymer

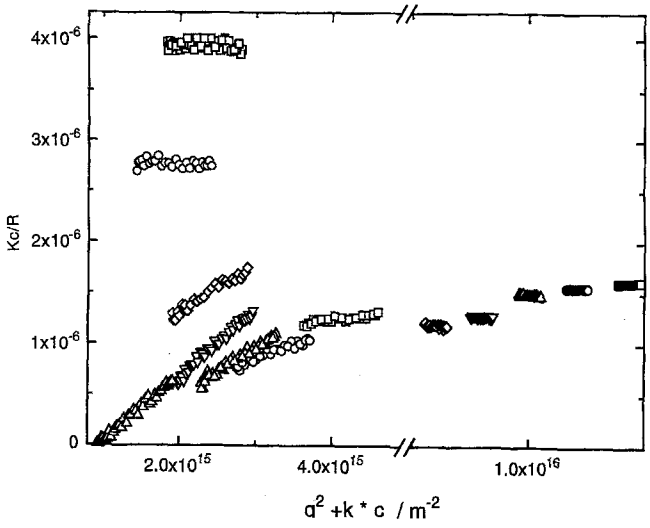


**Fig. 5** Static Zimm plot of the series D at $T = 20\,°C$ ($k = 5\,10^{16}\,cm^3g^{-1}m^{-2}$)

concentration is observed. At low droplet concentrations the osmotic modulus decreases with decreasing $c_{nd}$. The crossing over occurs at a concentration where the inter-droplet distance becomes comparable with the mean end-to-end distance of the polymer. For $c_p = 7\,10^{-3}$ g/cm$^3$ a maximum in the osmotic modulus is found at $c_{nd} = 0.036$ g/cm$^3$. At this concentration the sample shows also a maximum in the viscosity and a weak gelation. A detailed discussion of this behavior follows below.

The scattered intensity of the pure microemulsion shows a maximum at about $c_{nd} = 0.03$ g/cm$^3$, i.e., the osmotic modulus first decreases with droplet concentration and then increases. This is a well known behavior for w/o microemulsions [17] and is explained by a combined hard sphere repulsive and a short ranged attractive potential due to van der Waals attraction and interpenetration of the surface layer of opposite particle surfaces.

The analysis of the intensity autocorrelation function $g^2(t)$ for the diluted samples yields two dominating correlation processes which are both $q^2$-dependent. The constants of the fast diffusion process were plotted against $c_{nd}$ in Fig. 7. In analogy to the osmotic modulus a monotonical increase of the diffusion constants is observed with increasing polymer concentration in the high concentration regime. For $c_p < 0.07$ g/cm$^3$ the diffusion constants decrease the stronger the higher the polymer concentration. The microemulsion without polymer shows the dominant attractive interaction at low droplet concentrations and a diffusion constant of $4.1\,10^{-11}\,m^2s^{-1}$ is extrapolated for $c_{nd} = 0$. From the Stokes–Einstein relation ($D = kT/6\pi\eta R_h$) a hydrodynamic radius of 9.8 nm is obtained which agrees reasonably with the radius of the nanodroplet. The diffusion constant of the slow process is plotted against $c_{nd}$ in Fig. 8. It decreases with increasing polymer concentration. This behavior is much less pronounced than the decrease of the diffusion coefficient by orders of magnitude with decreasing droplet concentration. At first sight this is a surprising effect but it will shed some light on the nature of the slow correlation process.

## Discussion

### Diffusion processes obtained by QELS

In the pure microemulsion the diffusion process arises from the collective compression-dilatation motions of the nanodroplets [18]. Addition of polymer leads to an increase of the osmotic modulus (see Fig. 6) and, therefore, to an increase of the collective diffusion coefficient. Comparison of the diffusion coefficients of the fast process in the pure and polymer containing microemulsions (Figs. 2 and 7, above 0.1 g/cm$^3$) reveals that both processes originate from the collective droplet motion. This was also concluded for the ABA triblock-copolymer microemulsion systems [5].

As regards the mechanism responsible for the slow diffusion process, this is a much more difficult question. At least two different molecular interpretations can be offered: the simplest idea is the droplet cluster formation via bridging polymer molecules leading to larger objects which are responsible for the slow diffusion process. This should result in a strong forward scattering which is observed only for very low nanodroplet concentrations. Previous studies with ABA triblock copolymers in the same w/o microemulsions showed that the slow diffusion process can be related to the polymer self diffusion [5]. Hence the molecular motion of the polymer chains is monitored by the nanodroplet scattering, since the contribution of the polymer chains to the scattering intensity is negligible. Calculating the ratio of the product of the optical contrast factor $K$ (using the values of the refractive index increment of the two component system polymer/oil and the quasi two-component system nanodroplet/oil) and $M_w$ of the nanodroplets and the polymer one yields a ratio of the scattering intensities of the nanodroplets to that of the polymer at equal concentrations of both components of about 1000. At higher droplet concentration it becomes still larger.

To approach a possible answer to the question of the responsible molecular process we summarize the experimental facts known about the slow process:

- the slow process becomes slower with increasing $c_p$ at $c_{nd} = \text{const.}$ (Fig. 2) and with decreasing $c_{nd}$ at $c_p = \text{const.}$ (Fig. 8),

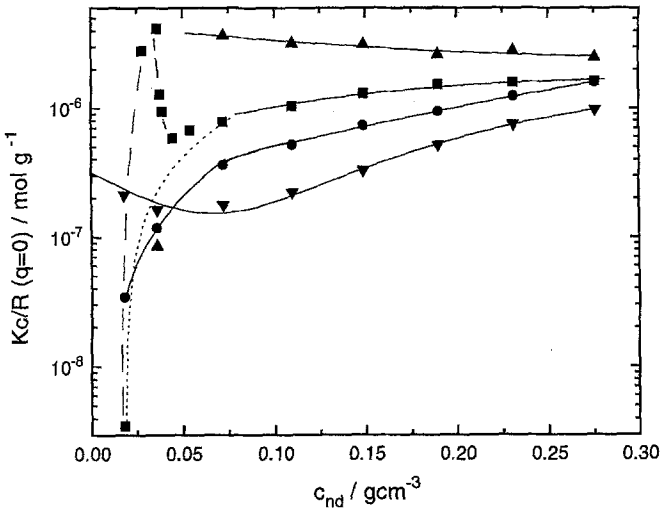


**Fig. 6** Osmotic modulus against droplet concentration for different polymer concentrations (▼ $c_p = 0$, ● $c_p = 0.003$ g/cm$^3$, ■ $c_p = 0.007$ g/cm$^3$, ▲ $c_p = 0.021$ g/cm$^3$). Full lines represent fitted curves, the short dashed line represents depletion model for series D and the long dashed line is a guide for the eye only

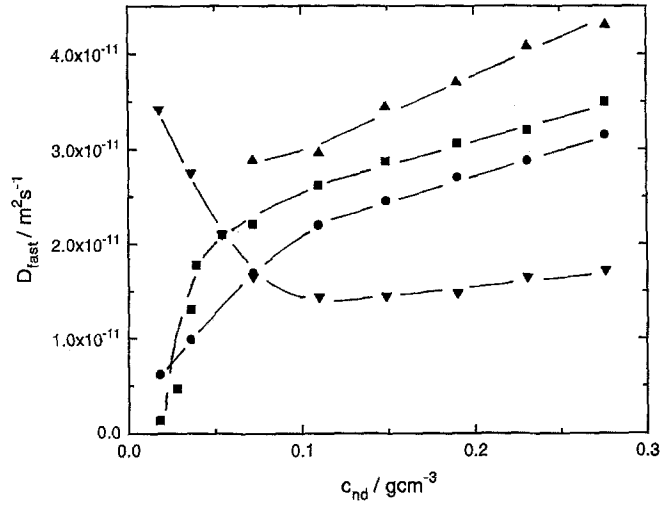


**Fig. 7** Nanodroplet concentration dependence of the fast diffusion process at different polymer concentrations (▼ $c_p = 0$, ● $c_p = 0.003$ g/cm$^3$, ■ $c_p = 0.007$ g/cm$^3$, ▲ $c_p = 0.021$ g/cm$^3$). Lines are guides for the eye

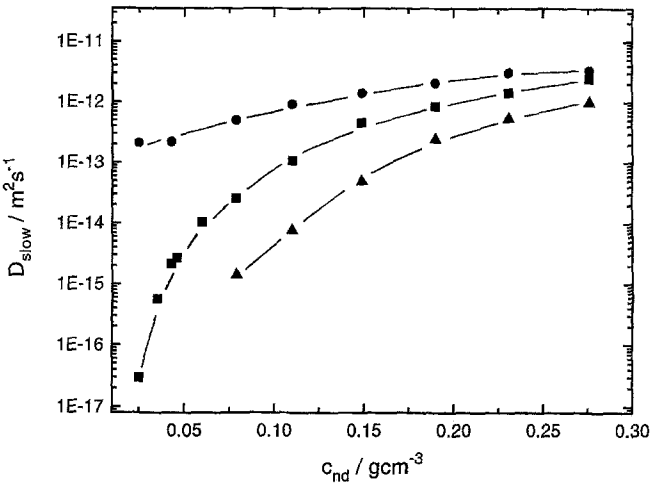


**Fig. 8** Nanodroplet concentration dependence of the slow diffusion process for different polymer concentrations (● $c_p = 0.003$ g/cm$^3$, ■ $c_p = 0.007$ g/cm$^3$, ▲ $c_p = 0.021$ g/cm$^3$). Lines are guides for the eye

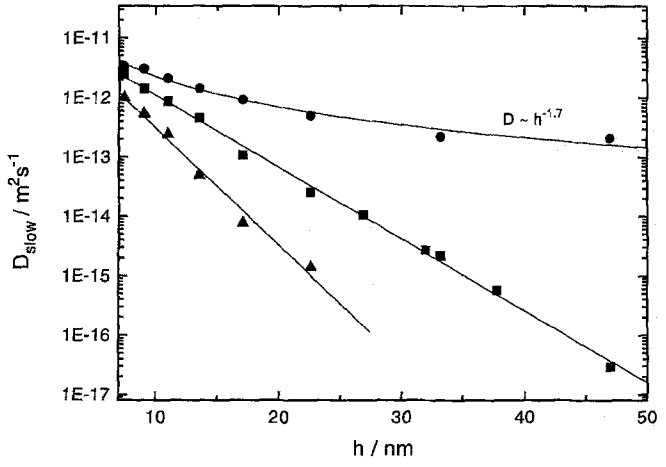


**Fig. 9** Slow diffusion coefficient against the interdroplet distance $h$ for different polymer concentrations (● $c_p = 0.003$ g/cm$^3$, ■ $c_p = 0.007$ g/cm$^3$, ▲ $c_p = 0.021$ g/cm$^3$). The dashed line represents a power law fit. The full lines show an exponential dependence on $h$

- the scattering intensity of the slow process is angular dependent. If only the particle form factors are responsible for the $q$-variations of the autocorrelation function one derives from a semi-logarithmic plot of the amplitude ratio against $q^2$ a correlation length of about 30–50 nm. This value agrees with the mean center to center distance between the nanodroplets
- the slow process becomes faster in the system spanning cluster regime, i.e., while building up of the dynamic droplet cluster (Fig. 3),
- the slow process vanishes if the polymer refractive index is crudely matched by that of the oil phase (Fig. 4).

The two last observations are not compatible with the idea of cluster formation due to the added polymer. We therefore suppose that the slow process originates from polymer concentration fluctuations. Such fluctuations result in a spatial inhomogeneous refractive index of the continuous phase surrounding the nanodroplets. This leads to a spatial distribution of the droplet scattering power even at spatially constant droplet concentration. Thus, the fast diffusion process is due to averaging the concentration fluctuations of the nanodroplets via

collective droplet motion. But this process does not lead to a complete decorrelation or the scattered light and the remaining correlation of scattered light is caused by the inhomogeneities of the scattering power of the spheres. This part of the correlation decays only by decaying of the fluctuations of the refractive index of the background, i.e., of the polymer solution. This picture is similar to that used to explain the slow mode obtained for interacting polydisperse spheres [18], with the exception that in our case the polydispersity fluctuations do not decay by the self-diffusion of the droplets. By contrast they decay due to the collective diffusion of the polymer chains which should be comparable to the self-diffusion, since we study the dilute polymer concentration regime. The polymer diffusion is strongly affected by the attractive interactions between the polar end groups of the polymer chain and the nanodroplets. As shown in ref. [19], we suppose that the contact time of the polar end group in the surfactant layer of the nanodroplet is the dominant factor controlling the diffusion of the polymer chain. This contact time strongly depends on the collision rate and contact time of two nanodroplets during collision between the droplets. With increasing collision rate and contact time the exchange of the chain end groups between two droplets or between one droplet and the oil phase (and vice versa) increases, leading to a faster polymer diffusion. This explains qualitatively the observed increase of the slow diffusion constant at the system spanning cluster formation (due to increasing contact time between the nanodroplets) and the decrease with dilution of the microemulsion, i.e., with increasing droplet distance (due to decreasing collision rate between the nanodroplets).

The above model implies that the interdroplet distance is the controlling parameter of the slow diffusion process (as shown in Fig. 8). For $c_p = 0.003$ g/cm$^3$ a power law dependence is observed with an exponent of $-1.7 \pm 0.2$. At larger concentrations the diffusion coefficient shows an exponential dependence. The crossing over coincides with the formation of a three-dimensional network. The onset of this network formation is controlled by the functionality of the droplets which depends on $R$.

## Concentration dependence of the osmotic modulus

At large $c_{nd}$ where the interdroplet distance is small compared to the end-to-end distance of the polymer chains, the addition of polymer increases the osmotic modulus. It is a consequence of an increasing repulsion between the droplets because of steric effects of the polymer brushes covering the droplets. At these small interdroplet distances the majority of the polymer end groups are attached to the surfactant layer of the droplets. Also, the bridging of the nearest neighbor droplets via the polymer chains would result in a compression of the polymer chain (i.e., bridging is preferred between droplets at larger distances than the nearest neighbor distance). Loop formation of one polymer chain over the surface of a nanodroplet seems likewise to be unfavorable, since the droplet diameter is smaller than the end-to-end distance of the polymer chain.

This situation changes at a certain droplet concentration, $c_{nd,c}$, where the interdroplet distance becomes comparable to the end-to-end distance of the PI chain. Theoretical investigations on polymer brushes on planar and spherical surfaces [20] have shown that at surface separations larger than the end-to-end distance of the polymer chain the number of bridging chains decreases drastically in favor of loops, dangling ends and free chains in case of weakly adsorbed chains. The free chains exert an additional attractive force on the nanodroplets. This is caused by their concentration difference in the wedged gaps (between opposite nanodroplets) and in free solution resulting in an osmotic pressure difference ($\Delta\Pi$). $\Delta\Pi$ causes the observed decrease in the osmotic modulus at droplet concentrations below 0.08 g/cm$^3$ at $c_p =$ 0.003 g/cm$^3$. One can try to estimate roughly the contribution of the depletion mechanism to the osmotic modulus using the calculations of Richmond and Lal [21] and Vrij [15]. For interdroplet distances large compared to the radius of gyration $r_g$ of the polymer chain the following equation for the osmotic pressure difference is obtained:

$$\Delta\Pi/RT \cong \frac{8nr_g^2}{\pi N_A h^2}, \tag{1}$$

with $n$ the number density of free polymer chains in free solution, $N_A$ Avogadro's constant and $h$ the interdroplet distance (surface to surface), where we have to consider that $h$ is a function of $c_{nd}$:

$$h \cong \sqrt[3]{\frac{M_{nd}}{N_A c_{nd}}} - 2r_{nd}. \tag{2}$$

In order to calculate the scattering intensity contribution due to the depletion effect, we require the dependence of $n$ on the weighed-in concentration of ionomers and nanodroplets. This is accessible via an equilibrium association of ionomers ($P$) and nanodroplets ($D$), such that $v$ ionomers interact with one nanodroplet, i.e.,

$$vP + D \xleftrightarrow{K} DP_v. \tag{3}$$

Applying the mass action law, the mass balance and making some suitable approximations, one arrives at the number density of free ionomers,

$$n \cong \frac{N_A}{M_p} c_p \left[1 - \frac{a^2 c_{nd}^2}{1 + bc_{nd}}\right], \tag{4}$$

where $a = 1/c_p$, $b = (1 + c_p^v K)/(c_p^{v+1} K)$ and $M_p$ being the ionomer molecular weight. There exists a characteristic nanodroplet concentration $c_{nd,c}$ where $n = 0$, i.e., $c_{nd,c} \cong b/a^2$ provided $bc_{nd} \gg 1$, i.e., $c_p^v K \ll 1$. This condition conforms to the experimental situation. Thus, Eq. (4) can be given the form

$$n = \frac{N_A}{M_p} c_p \left[1 - \frac{c_{nd}}{c_{nd,c}}\right] \tag{5}$$

or after insertion of Eq. (5) into Eq. (1),

$$\Delta\Pi/RT \cong \frac{8c_p\left[1 - \frac{c_{nd}}{c_{nd,c}}\right]r_g^2}{\pi N_A h^2} . \tag{6}$$

Equation (5) conforms to Monte Carlo studies of telechelic polymer chains adsorbed onto flat parallel surfaces [22]. They show for surface separations larger than the mean end-to-end distance of the polymer chain that the amount of free polymer chains increases with increasing separation, i.e., with decreasing nanodroplet concentration. Also in case of curved interfaces the characteristic concentration $c_{nd,c}$ defines approximately that concentration where the interdroplet distance equals the end-to-end distance of the ionomer chain.

The contribution to the osmotic modulus is obtained by calculating the derivative of Eq. (1) with respect to the droplet concentration $c_{nd}$ and in the case $c_{nd} < c_{nd,c}$, one obtains:

$$\frac{1}{RT}\left[\frac{\delta\pi}{\delta c_{nd}}\right]_{dep} \approx -\frac{16r_g^2}{3\pi M_p}\left[\frac{N_A}{M_{nd}}\right]^{2/3} c_p\left[1 - \frac{c_{nd}}{c_{nd,c}}\right] \times \frac{c_{nd}^{-1/3}}{(1 - 2r_{nd}\sqrt[3]{(N_A c_{nd}/M_{nd})})^3} , \tag{7}$$

where we have neglected an additive contribution proportional to $c_{nd}^{2/3}$ vanishing for $c_{nd} \to 0$. At concentrations $> c_{nd,c}$ the contribution of the depletion mechanism is zero and the osmotic modulus is determined by the interaction potential between the nanodroplets. The osmotic modulus of interacting particles is usually described by a virial expansion of the form:

$$\frac{Kc}{R(q=0)} = \frac{1}{M_{nd}} + A_1 c_{nd} + A_2 c_{nd}^2 + \cdots . \tag{8}$$

The values of $A_1$ and $A_2$ were obtained from a fit of the experimental data at $c_{nd} > 0.1$ g/cm$^3$. Below this concentration the osmotic modulus is fitted by the sum of Eqs. (3) and (4), where $A_1$ and $A_2$ were fixed. One obtains $c_p = 1.6\ 10^3$ g/cm$^{-3}$ and $c_{nd,c} = 0.08$ g/cm$^3$, i.e., only about 40% of the weighed-in polymer chains contributes to the fraction of free chains for $c_{nd} = 0.018$ g/cm$^3$. The other part of the polymer chains exists as loops and dangling ends; this agrees reasonably well with ref. [22]. The onset of the depletion mechanism occurs at an interdroplet distance of about 20 nm which follows from $c_{nd,c}$ using Eq. (2). This is somewhat lower than the mean end-to-end distance of the PI-chain in a good solvent (about 30 nm). One reason for this discrepancy is probably the spherical structure of the adsorbing interface which results in a distribution of interfacial distances larger than the interdroplet distance calculated from $c_{nd}$. The dotted line in Fig. 6 corresponds to a data set with the same value of $c_{nd,c}$ and $c_p = 2.8\ 10^3$ g/cm$^{-3}$ yielding about 30% free polymer chains at the lowest droplet concentration of the series D.

The variation of the concentration dependence of the osmotic modulus above a certain polymer concentration can only be understood by assuming a preferred local structure at an interdroplet distance equal to the end-to-end distance of the polymer chain. The osmotic modulus shows a maximum at $c_{nd} = 0.036$ g/cm$^3$ and $c_p = 7\ 10^3$ g/cm$^3$. At this particular interdroplet distance a minimum of the free energy of interaction between polymer adsorbing nanodroplets occurs, thus defining a polymer nanodroplet aggregate characterized by bridging of nearest neighbor nanodroplets [20]. The polymer chains prefer apparently to accumulate between opposite droplets leading to a much stronger repulsion in case of compression of the droplets. Thus with increasing polymer concentration the repulsive force prevails over the depletion force at constant $c_{nd}$ (in the present case $c_{nd} \cong 0.036$ g/cm$^3$).

At this point, one has to note that the absolute values of $Kc/R_\theta$ at higher $c_p$ are influenced by the dependence of the optical contrast factor $K$ from the structure of the solution. Stable clusters of two or more droplets and polymers, i.e., scattering objects determined by a correlation length large compared to the droplet distance, with a composition such that its refractive index is equal to that of the oil are invisible for light scattering (optically matched). This composition corresponds to $c_p = 0.007$ g/cm$^3$ and $c_{nd} = 0.031$ g/cm$^3$ and to $c_p = 0.021$ g/cm$^3$ and $c_{nd} = 0.094$ g/cm$^3$ at the given droplet size. At $c_p = 0.021$ g/cm$^3$ no evidence for the occurrence of such clusters is seen in Fig. 6 (upper curve), whereas the maximum in the curve for $c_p = 0.007$ g/cm$^3$ indicates the occurrence of such clusters. In other words, we can conclude that cluster forming in these systems is forced in the vicinity of and below the equilibrium distance.

From the occurrence of an equilibrium distance it must be concluded that the samples with $c_{nd} < 0.036$ g/cm$^3$ are only metastable. However, during light scattering measurements no phase separation was detected, but on time scales of a few weeks a separation of an oil phase was observed. This appears reasonable since the system tries to

adopt its equilibrium state, i.e., the droplet concentration which corresponds to the polymer end-to-end distance.

**Acknowledgment** We are grateful to the Swiss National Science Foundation for financial support of this work.

## References

1. Goddard ED, Ananthapadmanabhan KP (1993) Interactions of Surfactants with Polymers and Proteins. CRC Press, Inc
2. Bakeev KN, Chugunov SA, Teraoka I, MacKnight WJ, Zezin AB, Kabanov VA (1994) Macromolecules 27:3926–3932; Geiger S, Mandel M (1989) J Phys Chem 93:4195
3. a) Struis RPWJ, Eicke H-F (1991) J Phys Chem 95:5989 b) Hilfiker R, Eicke H-F, Steeb Ch, Hofmeier U (1991) J Phys Chem 95:1478 c) Hilfiker R (1991) Ber Bunsenges Phys Chemie 95:1227 d) Zhou Z, Hilfiker R, Hofmeier U, Eicke H-F (1992) Progr Colloid & Polymer Sci 89:66 e) Quellet Ch, Eicke H-F, Gu Xu, Hauger Y (1990) Macromolecules 23:3347
4. Zölzer U, Eicke H-F (1992) J Phys II France 2:2207; Odenwald M, Eicke H-F, Meier W (1995) Macromolecules 28:5069
5. Stieber F, Hofmeier U, Eicke H-F, Fleischer G (1993) Ber Bunsenges Phys Chemie 97:812; Fleischer G, Stieber F, Hofmeier U, Eicke H-F (1994) Langmuir 10:1780
6. Russo PS (1987) Reversible Polymer Gels and Related Systems. ACS Symposium Series 350, American Chemical Society: Washington, DC
7. Halperin A, Tirrell M, Lodge TP (1992) Adv Polym Sci 100:31
8. Misra S, Nguyen-Misra M, Mattice WL (1994) Macromolecules 27:5037–5042
9. Tanaka F, Edwards SF (1992) J Non-Newtonian Fluid Mech 43:247–309
10. Kubik R (1983) Dissertation Universität Basel, p 32
11. Möller M, Mühleisen E, Omeis J (1990) In: Burchard W, Ross Murphey SB (eds) Physical Networks – Polymer and Gels. Elsevier Science London
12. Graessley WW (1980) Polymer 21:258
13. Polymer Handbook (1974) 2nd Ed J Wiley & Sons NY
14. Meier W (1994) Langmuir (accepted for publication)
15. Vrij A (1976) Pure & Appl Chem 48:471–483
16. Safran SA, Webman I, Grest S (1985) Phys Rev A 32:506; Eicke H-F, Hilfiker R, Thomas H (1986) Chem Phys Lett 125:295
17. Caponeti E, Magid LJ (1989) In: Martelluci S, Chester AN (eds) Progress in microemulsion. Ettore Majorana International Science Series 41:185–206; Hou MJ, Kim M, Shah DO (1988) J Coll Interf Sci 123:398–412
18. Pusey PN (1991) In: Hansen JP, Levesque D, Zinn-Justin J (eds) Colloidal Suspensions NATO ASI Les Houches Session L1 1989 Liquids, Freezing and Glass Transition. Elsevier Sci Publ BV pp 763–942
19. Baxandell LG (1989) Macromolecules 22:1982
20. Semenov AN, Joanny J-F, Khokhlov AR (1995) Macromolecules 28: 1066–1075
21. Richmond P, Lal M (1974) Chem Phys Lett 24:594
22. Misra S, Mattice WL (1994) Macromolecules 27:2058–2065